The Astrophysical Journal Letters, 856:L9 (7pp), 2018 March 20 https://doi.org/10.3847/2041-8213/aab433

Infrared Spectroscopy of Carbonaceous-chondrite Inclusions in the Kapoeta Meteorite: Discovery of Nanodiamonds with New Spectral Features and Astrophysical Implications

Yassir A. Abdu[1], Frank C. Hawthorne[2], and Maria E. Varela[3]
[1] Department of Applied Physics and Astronomy, University of Sharjah, P.O. Box 27272, Sharjah, United Arab Emirates; yabdu@sharjah.ac.ae
[2] Department of Geological Sciences, University of Manitoba, Winnipeg, MB R3T 2N2, Canada
[3] Instituto de Ciencias Astronómicas de la Tierra y del Espacio (ICATE) Avenida España 1512 sur, J5402DSP, San Juan, Argentina
Received 2018 January 11; revised 2018 March 1; accepted 2018 March 3; published 2018 March 20

Abstract

We report the finding of nanodiamonds, coexisting with amorphous carbon, in carbonaceous-chondrite (CC) material from the Kapoeta achondritic meteorite by Fourier-transform infrared (FTIR) spectroscopy and micro-Raman spectroscopy. In the C–H stretching region (3100–2600 cm^{-1}), the FTIR spectrum of the Kapoeta CC material (KBr pellet) shows bands attributable to aliphatic CH_2 and CH_3 groups, and is very similar to IR spectra of organic matter in carbonaceous chondrites and the diffuse interstellar medium. Nanodiamonds, as evidenced by micro-Raman spectroscopy, were found in a dark region (~400 μm in size) in the KBr pellet. Micro-FTIR spectra collected from this region are dramatically different from the KBr-pellet spectrum, and their C–H stretching region is dominated by a strong and broad absorption band centered at ~2886 cm^{-1} (3.47 μm), very similar to that observed in IR absorption spectra of hydrocarbon dust in dense interstellar clouds. Micro-FTIR spectroscopy also indicates the presence of an aldehyde and a nitrile, and both of the molecules are ubiquitous in dense interstellar clouds. In addition, IR peaks in the 1500–800 cm^{-1} region are also observed, which may be attributed to different levels of nitrogen aggregation in diamonds. This is the first evidence for the presence of the 3.47 μm interstellar IR band in meteorites. Our results further support the assignment of this band to tertiary CH groups on the surfaces of nanodiamonds. The presence of the above interstellar bands and the absence of shock features in the Kapoeta nanodiamonds, as indicated by Raman spectroscopy, suggest formation by a nebular-condensation process similar to chemical-vapor deposition.

Key words: dust, extinction – infrared: ISM – ISM: molecules – meteorites, meteors, meteoroids

1. Introduction

Carbon is one of the most abundant elements in the interstellar medium, and it occurs in different forms, including hydrocarbon dust, graphite, amorphous carbon, and diamonds. Interstellar or presolar nanodiamonds were first discovered in the acid-treated residues of carbonaceous chondrites (Lewis et al. 1987), although their existence in the interstellar medium was predicted earlier by Saslaw & Gaustad (1969). These nanodiamonds have a mean crystallite size of 1–3 nm (Lewis et al. 1987; Daulton et al. 1996) and they contain isotopically anomalous noble gases, particularly a Xe-HL anomaly, where the diamond is enriched both in the heavy (H) and the light (L) isotopes of Xe (Lewis et al. 1987). They also contain isotopically anomalous N that is enriched in ^{14}N (Russell et al. 1996). The presence of the Xe-HL noble-gas component indicates that at least a fraction of meteoritic diamonds has a supernova-related origin (Braatz et al. 2000). However, some meteoritic diamonds may have formed within the inner solar system (Dai et al. 2002).

Infrared spectra of some dense interstellar clouds show a broad absorption feature centered at ~2880 cm^{-1} (3.47 μm) that was first detected by Allamandola et al. (1992, 1993). They assigned the IR feature to tertiary CH groups and proposed the carrier to be a diamond-like material. This assignment has been supported by theoretical calculations (Bauschlicher et al. 2007) and laboratory IR measurements of diamondoid molecules (Pirali et al. 2007) and carbon nanoparticles irradiated with H atoms (Mennella 2008). An alternative assignment for the 3.47 μm feature has been suggested by Dartois et al. (2002) who assigned it to an OH stretch of H_2O bonded to NH_3 by a strong hydrogen bond. In emission spectra, Guillois et al. (1999) compared the IR features at 3.43 and 3.53 μm in spectra of the Herbig Ae/Be stars, HD 97048 and Elias 1, to laboratory spectra of synthetic hydrogenated diamonds, and assigned them to CH_x groups on the surface of nanodiamond particles $\geqslant$50 nm (Guillois et al. 1999).

The above interstellar features have not been reported before in IR spectra of meteoritic nanodiamonds (e.g., Lewis et al. 1989; Colangeli et al. 1994; Mutschke et al. 1995; Hill et al. 1997; Andersen et al. 1998). In fact, the IR spectra of these nanodiamonds are dominated by many artifacts due to surface adsorbates resulting from the chemical treatment used to isolate them from carbonaceous meteorites (Mutschke et al. 1995; Braatz et al. 2000).

Kapoeta is an achondrite meteorite that belongs to the howardite group. It is characterized as a gas-rich polymict breccia, and contains mm-sized dark inclusions that are described as carbonaceous-chondrite (CC) materials (Zolensky et al. 1996). In this letter, we report the finding of nanodiamonds, coexisting with amorphous carbon, in the CC material from the Kapoeta meteorite. We provide the first evidence for the presence of the 3.47 μm IR band, and other interstellar bands, in meteorites.

2. Experiment

FTIR spectra on a standard KBr pellet of the Kapoeta CC material (sample/KBr ratio is ~1%) were collected using a Bruker Tensor 27 FTIR spectrometer equipped with a KBr beam splitter and a DLATGS detector. Transmission micro-FTIR spectra on selected areas in the KBr pellet (spot size is ~50–100 μm) were acquired with a Bruker Hyperion 2000 IR microscope equipped with a liquid-nitrogen-cooled mercury

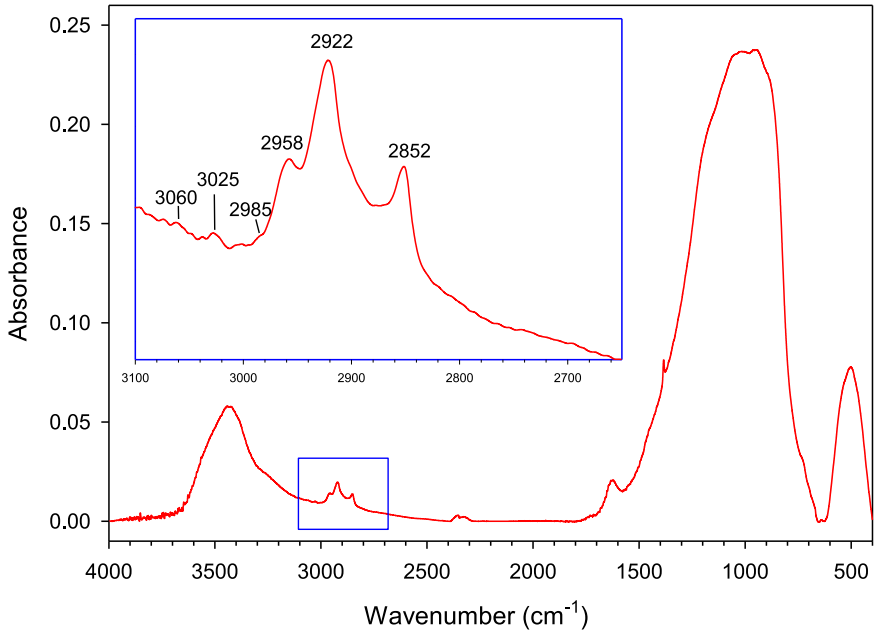

Figure 1. FTIR spectrum of the Kapoeta carbonaceous-chondrite material (KBr pellet). Inset: magnification of the C–H stretching region.

cadmium telluride (MCT) detector. Spectra over the range of 4000–400 cm^{-1} (2.5–25 μm), 4000–650 cm^{-1} (2.5–15.4 μm) for micro-FTIR, were obtained by averaging 100 scans with a resolution of 4 cm^{-1}. Base-line correction was done using the OPUS spectroscopic software (Bruker Optic GmbH).

Micro-Raman spectroscopy measurements were done using a LabRAM ARAMIS confocal microscope (Horiba Jobin Yvon) equipped with a 460 mm focal-length spectrograph and a multichannel air-cooled (−70°C) charge-coupled device (CCD) detector. A 100x objective microscope was used to focus the laser beam (532 nm excitation line) on the sample to a size of ~1 μm. The wavenumber was calibrated using the 520.7 cm^{-1} line of Si metal. The Raman spectra were analyzed using the LabSpec5 software package. All experimental work was done in the Department of Geological Sciences, University of Manitoba, Canada.

3. Results and Discussion

3.1. FTIR Spectroscopy

Figure 1 shows the KBr-pellet FTIR spectrum of the Kapoeta CC material. It consists of a strong and broad absorption band at ~1000 cm^{-1} (10 μm) due to Si–O stretches in silicates, with Si–O–Si bends occurring at ~500 cm^{-1} (20 μm), a triplet centered at ~2900 cm^{-1} (3.4 μm) originating from C–H stretches in hydrocarbons, and H_2O stretch and bend bands at ~3400 cm^{-1} (2.94 μm) and 1630 cm^{-1} (6.13 μm), respectively. Heating of the KBr pellet in a desiccator oven at ~105°C for ~10 hr significantly reduced the intensity of the H_2O bands, indicating that these bands are mostly from H_2O absorbed by KBr. The sharp peak at 1384 cm^{-1} (7.23 μm) (Figure 1) is an artifact from the KBr matrix. The absence of sharp OH-stretching peaks in the 3700–3600 cm^{-1} (2.7–2.8 μm) region indicates that this CC material is dominated by anhydrous silicates, and the broad and featureless Si–O stretching band at 1000 cm^{-1} (10 μm) suggests that the silicates are amorphous or poorly crystalline (Figure 1).

The C–H stretching region (3100–2600 cm^{-1}) (3.2–3.8 μm) of the KBr-pellet spectrum (inset to Figure 1) is dominated by a strong absorption band at ~2922 cm^{-1} (3.42 μm) due to asymmetric stretches of the CH_2 groups, with their symmetric stretches observed at ~2852 cm^{-1} (3.51 μm). The band at ~2958 cm^{-1} (3.38 μm) is due to CH_3 asymmetric stretches. Very weak bands/shoulders at ~2985 cm^{-1} (3.35 μm) and 3002 cm^{-1} (3.33 μm) may be assigned to olefinic CH_x stretches, and at ~3025 cm^{-1} (3.31 μm) and 3060 (3.27 μm) cm^{-1} to C–H stretches in aromatic hydrocarbons.

3.2. Raman Spectroscopy

Visual inspection of the KBr pellet of the Kapoeta CC material shows the existence of a very dark region ~400 μm in size, referred to hereafter as the diamond-enriched region. A scan of this region using a CCD camera attached to the Raman microscope revealed the presence of highly reflecting micro- to submicrometer particles forming clusters that scatter in and around the region. One of these clusters is shown in Figure 2. Figure 3 shows representative Raman spectra (1000–2000 cm^{-1}) taken from the cluster of particles in Figure 2. In Figure 3(a), the sharp peak centered at 1333 cm^{-1} is characteristic of the first-order Raman line of diamond and the broad peaks centered at ~1360 and 1600 cm^{-1} are the D- and G-bands, respectively, of amorphous carbon (Knight & White 1989). The two broad features at ~1150 and 1450 cm^{-1} are usually seen in spectra of chemical-vapor-deposition (CVD) nanodiamonds, and the former has been used by some authors as an indication for the existence of nanodiamonds (Zhou et al. 1998; Popov et al. 2004). Ferrari & Robertson (2001) assigned both peaks to transpolyacetylene at grain boundaries and surfaces of nanodiamonds. The weak peak at ~1020 cm^{-1} along with the broad feature centered at ~1270 cm^{-1} are also associated with nanodiamonds (Veres et al. 2007; May et al. 2008), and the broad doublet at ~1800 and 1900 cm^{-1} may be due to overtones and/or combinations. In the 2000–4000 cm^{-1} region (not shown), the Raman spectra show broad CH-stretching peaks centered at ~2900 cm^{-1} in

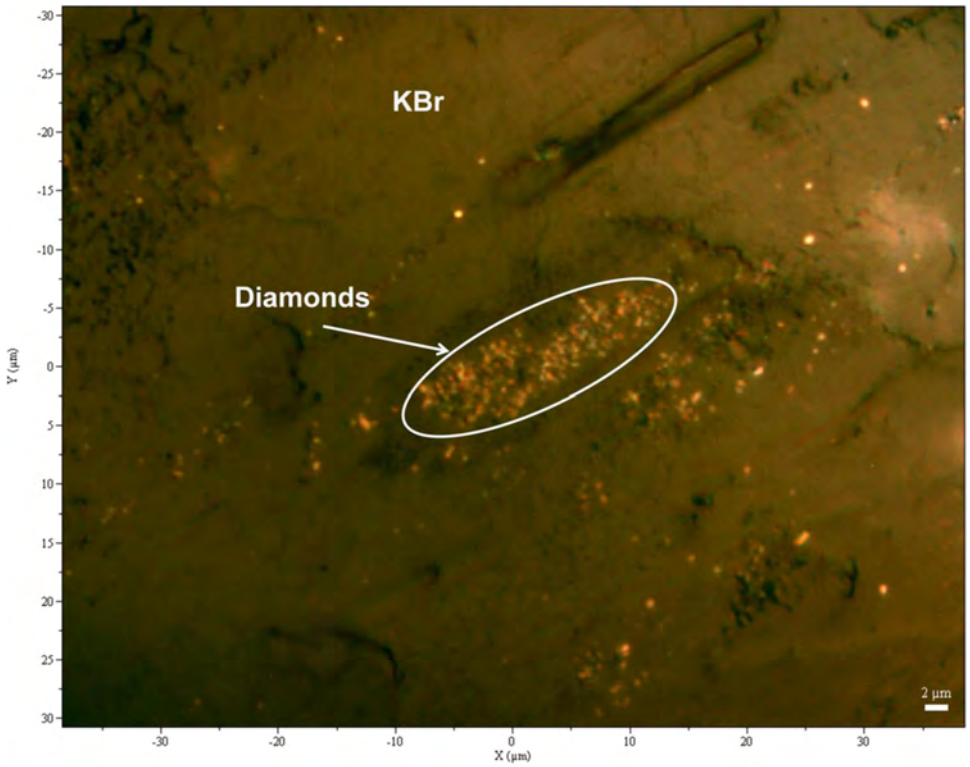

Figure 2. Reflected-light image from the KBr pellet of the Kapoeta carbonaceous-chondrite material showing a cluster of diamond particles.

addition to the second-order peaks of nanodiamonds and graphitic/amorphous carbon.

Thus, in the cluster of particles shown in Figure 2, each particle may be considered as an aggregate of nanodiamonds. To estimate the sizes of these nanodiamonds from their Raman spectra, we consider the particle-size dependence of the position and FWHM of the 1333 cm^{-1} diamond peak (Yoshikawa et al. 1993). Based on the analyses of 26 Raman spectra, the average diamond peak position and FWHM are 1332.6 cm^{-1} ($\sigma = 0.3\ cm^{-1}$) and 4.0 cm^{-1} ($\sigma = 0.6\ cm^{-1}$), respectively, suggesting a particle size of $\geqslant$50 nm for the Kapoeta diamonds that show the Raman diamond peak in their spectra. However, some spectra do not show the Raman diamond peak at 1333 cm^{-1}, but they display all the other peaks shown in Figure 3(a), including the peaks and features associated with nanodiamonds at ~1020, 1150, 1450 cm^{-1}, and ~1270 cm^{-1} (Figure 3(b)). The spectrum shown in Figure 3(b) is very similar to the Raman spectra of ultrananocrystalline diamonds having an average particle size of ~3–5 nm, i.e., single-digit nanodiamonds, where the 1333 cm^{-1} diamond peak is absent and they show the D- and G-bands along with the 1150 and 1450 cm^{-1} peaks (Popov et al. 2004). One difference is that the G-band in their spectra occur at a lower wavenumber (1560 cm^{-1}), possibly due to differences in sp^2/sp^3 ratios in the amorphous carbon phase. Thus, our Raman spectroscopic data suggest the existence of two populations of nanodiamonds in the Kapoeta CC material: nanodiamonds that are $\geqslant$50 nm and single-digit nanodiamonds.

3.3. Micro-FTIR Spectroscopy

Figure 4(a) shows a typical micro-FTIR spectrum taken from the diamond-enriched region (spot size is ~70 μm). It is dramatically different from the KBr-pellet spectrum (Figure 1) both in the high- and low-frequency sides. The position of the absorption bands and their possible assignments are listed in Table 1.

3.3.1. C–H Stretching Bands

The C–H stretching region of the FTIR spectrum of the diamond-enriched region (Figure 4(b)) is dominated by a broad and intense band at ~2886 cm^{-1} (~3.47 μm), which may be assigned to tertiary CH groups (Smith 1999) on the surfaces of nanodiamonds. Allamandola et al. (1992, 1993) observed a broad and intense absorption band centered at ~3.47 μm in the IR spectra of hydrocarbon dust in dense molecular clouds. They tentatively assigned the band to tertiary CH stretches and suggested the carrier, which is a ubiquitous component of dense clouds, to be a diamond-like material. This band has been identified in IR spectra of synthetic diamondoid molecules (Pirali et al. 2007) and as a weak feature in IR spectra of laboratory-produced hydrogenated amorphous carbon (Grishko & Duley 2000). It has also been activated in IR spectra of carbon nanoparticles irradiated by H atoms under simulated dense-medium conditions (Mennella 2008). The 3.47 μm band has not been identified before in IR spectra of meteoritic nanodiamonds isolated from carbonaceous meteorites. This could be due to the chemical treatment used during the isolation process, especially oxidation processes, which could destroy the H-terminations on nanodiamond surfaces (Braatz et al. 2000). However, the Kapoeta nanodiamonds studied here are pristine and have not been treated chemically. Our IR spectroscopic results provide the first evidence for the existence of the 3.47 μm interstellar band in meteorites, and further support the suggestion of Allamandola et al. (1992, 1993) that the band is due to a diamond-like material.

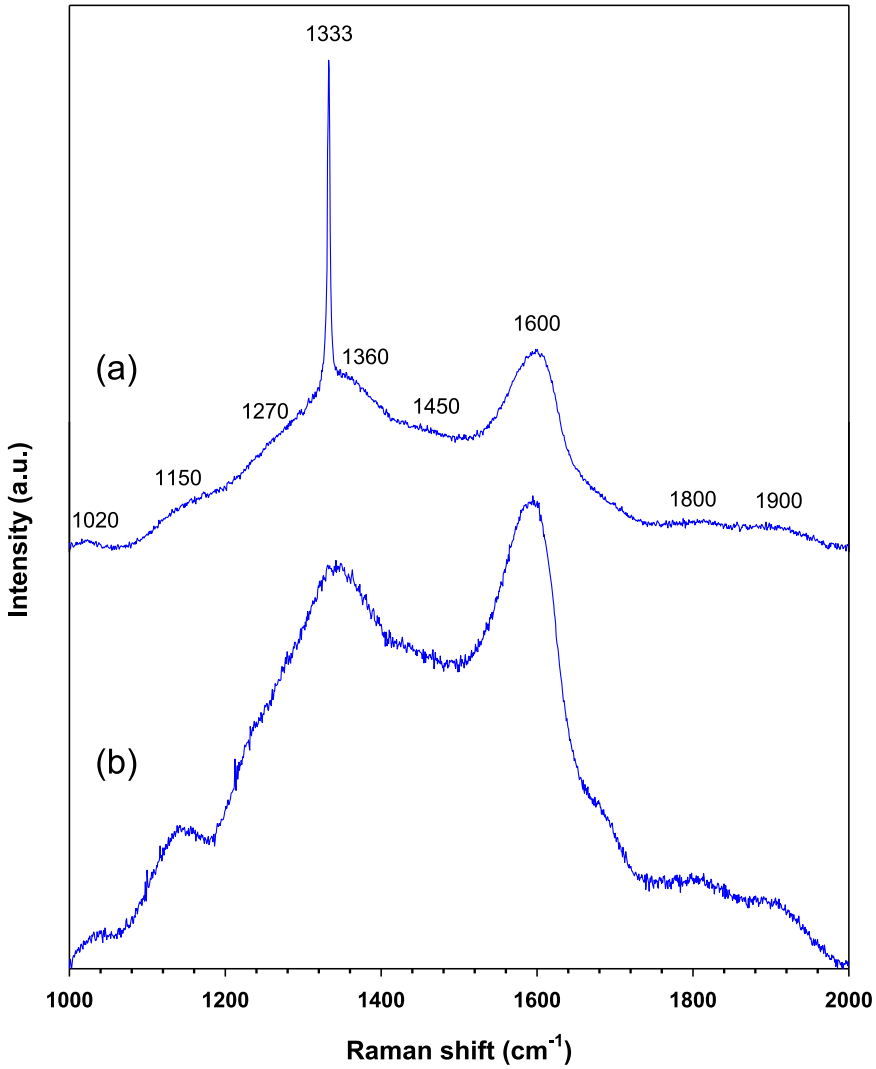

Figure 3. Raman spectra of the Kapoeta nanodiamonds (see the text for details).

The bands at 2920 and 2860 cm^{-1} are due to CH_2 stretches and that at 2945 cm^{-1} to CH_3 stretches (Table 1), and all of them occur as shoulders on the 2886 cm^{-1} band (Figure 4(b)). We observe the bending vibrations of these groups at 1468 cm^{-1} (CH_3 bend) and 1455 cm^{-1} (CH_2 bend). The observed CH_2 and CH_3 bands are not expected to be seen in IR spectra of single-digit nanodiamonds, because of their small domain sizes (Cheng et al. 2005). However, the 2945, 2920, and 2860 cm^{-1} bands (Figure 4(b)) are in close agreement with those reported for CH_x groups on the surface of a 100 nm diamond (Jones et al. 2004).

In addition to the above CH_2 and CH_3 bands, there is a clear shoulder at ~2805 cm^{-1} and a less-obvious shoulder at ~2830 cm^{-1} (Figure 4(b)) that we may assign to C–H stretching vibrations of a CH_3 group attached to N and O, respectively (Smith 1999). Bands assigned to CH_3 stretches in N–CH_3 and O–CH_3 groups have been reported in IR spectra of nitrogenated chemical vapor deposited (CVD) diamond films (McNamara et al. 1994). The pair of sharp peaks at 2740 and 2695 cm^{-1} (Figure 4(b)) are characteristic of aldehydic C–H stretches (Smith 1999). This assignment is further supported by the presence of a C=O stretch band at 1732 cm^{-1} (Table 1). The location of the 2695 cm^{-1} peak is consistent with an α-C being quaternary (Smith 1999), suggesting that the aldehyde group is on the surface of nanodiamonds. The weak band at 3025 cm^{-1} is due to C–H stretches in aromatic hydrocarbons.

3.3.2. Nitrogen-related Bands and Other IR Features

The C≡N stretching band in saturated nitriles occurs at 2260–2240 cm^{-1} and that of aromatic nitriles at 2240–2220 cm^{-1} (Smith 1999). We observe the C≡N band at 2237 cm^{-1} (see the inset of Figure 4(a)), which falls in the range of aromatic nitriles. Nitriles and aldehydes, which are abundant interstellar molecules, have been identified in meteoritic organic matter by pyrolysis techniques (e.g., Sephton 2012), but their IR spectroscopic features are shown here for the first time. The inset of Figure 4(a) also shows a weaker peak at 2165 cm^{-1} (4.62 μm), which matches the interstellar band seen in IR spectra of some protostars embedded in dense molecular clouds (Pendleton et al. 1999). We assign this peak along with the broad feature at 1965 cm^{-1} (Figure 4(a); Table 1) to CO adsorbed on the surface of nanodiamonds. Bands in the 2200–1900 cm^{-1} region have been attributed to CO adsorbed on the surfaces of some transition metal nanoparticles (Blizanac et al. 2004; Ivanova et al. 2007).

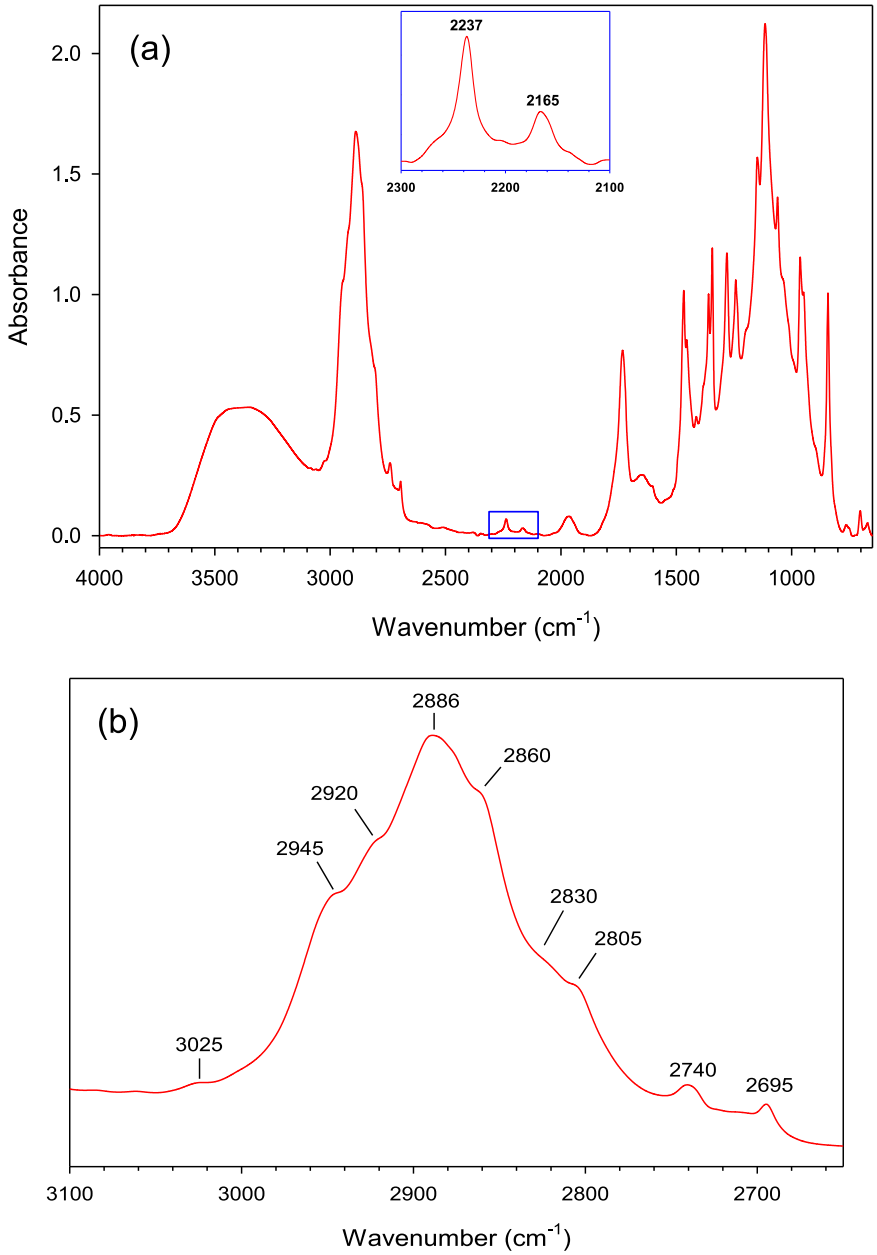

Figure 4. (a) Micro-FTIR spectrum collected from the diamond-enriched region in the KBr pellet of the Kapoeta carbonaceous-chondrite material (see the text for details). (b) Expanded view of the C–H stretch region.

Nitrogen impurities in diamonds induce characteristic IR absorption features that depend on the type of N-substitution (Evans & Qi 1982). For example, natural diamonds with singly substituted N atoms are called type Ib diamonds and diamonds with N in various forms of aggregate are termed type Ia diamonds. Nitrogen is the most common substitutional trace element in meteoritic nanodiamonds where it occurs in amounts up to ~1 wt% (Russell et al. 1996). Following the Raman work on boron-doped films (Niaura et al. 2009) where the appearance of Raman bands near 1165–1300 cm^{-1} has been attributed to the presence of boron in the film, we may infer the presence of nitrogen in the Kapoeta nanodiamonds from the observation of the Raman features near 1270–1300 cm^{-1} (Figure 3).

The sharp peak at 1344 cm^{-1} and the relatively broad peak at 1148 cm^{-1} (Table 1) may be assigned to a single substitutional N atom in the diamond structure (Kiflawi et al. 1994). The presence of a CH_3 group attached to N (Table 1) is in accord with this assignment, and suggests that the N-substitution occurs close to the surface of nanodiamonds. This is in agreement with theoretical calculations on substitutional N in nanodiamonds where it is predicted that N is likely to be located near the surface of the nanodiamond (Barnard & Sternberg 2005). The peak at 1280 cm^{-1}, along with the broad feature at ~1200 cm^{-1}, could be attributed to the presence of A-aggregates (i.e., a pair of N atoms) in the diamond structure, typical of type IaA diamonds (Evans & Qi 1982). The sharp peak at 1360 cm^{-1} may be due to platelet N (Kiflawi et al. 1998) or a CH_3 bend. The peaks at 1115, 1045, and 950 cm^{-1} may be assigned to positively charged substitutional N (N^+) (Lawson et al. 1998), possibly as a result of irradiation. There is

Table 1
Assignment of IR Bands in FTIR Spectrum of the Diamond-enriched Region of the Kapoeta CC Material

Frequency (cm^{-1})	Assignment(s)
3400	NH_2/H_2O stretch
3025	Aromatic CH stretch
2945	Asym. CH_3
2920	Asym. CH_2
2886	Tertiary CH
2860	Sym. CH_2
2830	(O–)CH_3
2805	(N–)CH_3
2740	Aldehydic CH
2695	Aldehydic CH
2237	C≡N stretch
2165	CO
1965	CO
1732	C=O stretch
1650	NH_2/H_2O bend
1601	C=C stretch
1468	CH_3 bend
1455	CH_2 bend
1413	Aldehydic C–C stretch/oleph CH_2 bend
1360	Platelet N/CH_3 sym. bend
1344	Substitutional N°
1280	A-aggregate (pair of N)
1241	C–N stretch
1200	C–N stretch/diamond lattice mode
1148	Substitutional N°
1115	Substitutional N^+
1061	C–O–C
1045	Substitutional N^+
1035	?
962	?
950	Substitutional N^+
843	PAH

ample evidence in the literature on the irradiation of the Kapoeta material by cosmic rays from the early Sun (e.g., Hidaka & Yoneda 2014, and references therein).

The carbonaceous-chondrite inclusions (clasts) in the howardites, eucrites, and diogenites (HED) meteorites are of C2 matter, and include both mm-sized clasts (Zolensky et al. 1996) and submillimeter-sized clasts (Gounelle et al. 2003). The submillimeter-sized clasts (microclasts) have been considered as micrometeorites, rather than fragments of larger objects, which were probably incorporated into the HED asteroid(s) between the solar system birth and 3.4 Ga ago (Gounelle et al. 2003). Both microclasts and mm-sized clasts of C2 matter show evidence of heating, e.g., destruction of phyllosilicates in the CM2 and CR2 material suggesting peak temperatures on the order of 400°C, that was attributed to impact onto the HED asteroid (Zolensky et al. 1996). The question that arises is: can nanodiamonds in Kapoeta be produced by shock-induced transformation of carbonaceous matter in a late-impact process that affected the howardite parent body? It is unlikely that the Kapoeta nanodiamonds were formed in this way. First, the 1150 and 1450 cm^{-1} Raman peaks (Figure 3) are not seen in the spectra of nanodiamonds produced by shock (Ferrari & Robertson 2001). Second, in shock-produced nanodiamonds, the first-order Raman peak of diamond suffers broadening and down shift (Ferrari & Robertson 2001), which are not observed in our spectra. These observations, along with the presence of the 3.47 μm IR band and other interstellar bands, suggest that nanodiamonds in Kapoeta may represent pristine matter—possibly formed by a nebular-condensation process (e.g., CVD)—trapped in the howardite parent body's regolith early in the history of the solar system.

We thank an anonymous referee for useful suggestions that improved the quality of the manuscript. This work was partially supported by a University of Sharjah seed grant (1702143047-P) to Y.A.A.

ORCID iDs

Yassir A. Abdu https://orcid.org/0000-0003-4432-6486
Frank C. Hawthorne https://orcid.org/0000-0001-6405-9931

References

Allamandola, L. J., Sandford, S. A., Tielens, A. G. G. M., & Herbst, T. M. 1992, ApJ, 399, 134
Allamandola, L. J., Sandford, S. A., Tielens, A. G. G. M., & Herbst, T. M. 1993, Sci, 260, 64
Andersen, A. C., Jorgensen, U. G., Nicolaisen, F. M., Sorensen, P. G., & Glejbol, K. 1998, A&A, 330, 1080
Barnard, A. S., & Sternberg, M. 2005, JPCB, 109, 17107
Bauschlicher, C. W., Jr., Liu, Y., Ricca, A., Mattioda, A. L., & Allamandola, L. J. 2007, ApJ, 671, 458
Blizanac, B. B., Arenz, M., Ross, P. N., & Markovic, N. M. 2004, JAChS, 126, 10130
Braatz, A., Ott, U., Henning, Th., Jager, C., & Jeschke, G. 2000, M&PS, 35, 75
Cheng, C.-L., Chen, C.-F., Shaio, W.-C., Tsai, D.-S., & Chen, K.-H. 2005, DRM, 14, 1455
Colangeli, L., Mennella, V., Stephens, J. R., & Bussoletti, E. 1994, A&A, 284, 583
Dai, Z. R., Bradley, J. P., Joswiak, D. J., et al. 2002, Natur, 418, 157
Dartois, E., d'Hendecourt, L., Thi, W., Pontoppidan, K. M., & van Dishoeck, E. F. 2002, A&A, 394, 1057
Daulton, T. L., Eisenhour, D. D., Bernatowlcz, T. J., Lewis, R. S., & Buseck, P. R. 1996, GeCoA, 60, 4853
Evans, T., & Qi, Z. 1982, RSPSA, 381, 159
Ferrari, A. C., & Robertson, J. 2001, PhRvB, 63, 121405(R)
Gounelle, M., Zolensky, M. E., Loiu, J-C., Bland, P. A., & Alard, O. 2003, GeCoA, 67, 507
Grishko, V. I., & Duley, W. W. 2000, ApJL, 543, L85
Guillois, O., Ledoux, G., & Reynaud, C. 1999, ApJL, 521, L133
Hidaka, H., & Yoneda, S. 2014, ApJ, 786, 138
Hill, H. G. M., d'Hendecourt, L. B., Perron, C., & Jones, A. P. 1997, M&PS, 32, 713
Ivanova, E., Mihaylov, M., Thibault-Starzyk, F., Daturi, M., & Hadjiivanov, K. 2007, J. Mol. Catal. A Chem., 274, 179
Jones, A. P., d'Hendecourt, L. B., Sheu, S.-Y., et al. 2004, A&A, 416, 235
Kiflawi, I., Bruley, J., Luyten, W., & van Tendleloo, G. 1998, PMagB, 78, 299
Kiflawi, I., Mayer, A. E., Spear, P. M., van Wyk, J. A., & Woods, G. S. 1994, PMagB, 69, 1141
Knight, D. S., & White, W. B. 1989, JMatR, 4, 385
Lawson, S. C., Fisher, D., Hunt, D. C., & Newton, M. E. 1998, JPCM, 10, 6171
Lewis, R. S., Anders, E., & Draine, B. T. 1989, Natur, 339, 117
Lewis, R. S., Ming, T., Wacker, J. F., Anders, E., & Steel, E. 1987, Natur, 326, 160
May, P. W., Smith, J. A., & Rosser, K. N. 2008, DRM, 17, 199
McNamara, K. M., Williams, B. E., Gleason, K. K., & Scruggs, B. E. 1994, JAP, 76, 2466
Mennella, V. 2008, ApJL, 682, L000
Mutschke, H., Dorschner, J., Henning, T. H., & Jager, C. 1995, ApJL, 454, L157
Niaura, G., Ragauskas, R., Dikcius, A., Sebeka, B., & Kuodis, Z. 2009, Chemija, 20, 78
Pendleton, Y. J., Tielens, A. G. G. M., Tokunaga, A. T., & Bernstein, M. P. 1999, ApJ, 513, 294
Pirali, O., Vervloet, M., Dahl, J. E., et al. 2007, ApJ, 661, 919

Popov, C., Kulisch, W., Gibson, P. N., Ceccone, G., & Jelinek, M. 2004, DRM, 13, 1371
Russell, S. S., Arden, J. W., & Pillinger, C. T. 1996, M&PS, 31, 343
Saslaw, W. C., & Gaustad, J. E. 1969, Natur, 221, 160
Sephton, M. A. 2012, MSRv, 31, 560
Smith, B. C. 1999, Infrared Spectral Interpretation: A Systematic Approach (Boca Raton, FL: CRC Press)
Veres, M., Tóth, S., & Koós, M. 2007, ApPhL, 91, 031913
Yoshikawa, M., Mori, Y., Maegawa, M., et al. 1993, ApPhL, 62, 3114
Zhou, D., Gruen, D. M., Qin, L. C., McCauley, T. G., & Krauss, A. R. 1998, JAP, 84, 1981
Zolensky, M. E., Weisberg, M. K., Buchanan, P. C., & Mittlefehldt, D. W. 1996, M&PS, 31, 518